

also valid for saturated hydrocarbons with labile hydrogen atoms.

As exhaust from lean-burn engines contains NO as the main NO_x component, the present knowledge could be technically implemented as a dual-catalyst system.^[21] On an oxidation catalyst such as Pt-ZSM-5, NO_x from a lean-burn exhaust stream can be converted into NO₂, which in turn is converted over an Ag/H zeolite catalyst. Injection of sufficient reducing agent between the two catalysts is required.

Experimental Section

In the experiment of Figure 1, the synthetic exhaust gas was composed of 400 ppm NO₂, 350 ppm propene, 350 ppm CO, 10% CO₂, 10% O₂, and 12% H₂O, balance helium. The volumetric hourly space velocity (VHSV) and the weight hourly space velocity (WHSV) were 160 000 h⁻¹ and 320 000 h⁻¹, respectively. NO, N₂O, and NO₂ were monitored by chemiluminescence and IR detectors. N₂ was monitored by gas chromatography.

In the experiment of Figure 2, the synthetic exhaust gas was composed of 450 ppm NO₂, 50 ppm NO, 175 ppm propene, 175 ppm propane, 350 ppm CO, 10% CO₂, 6% O₂, 12% water, balance helium. The VHSV was 60 000 h⁻¹.

Received: January 12, 1998 [Z11356IE]
German version: *Angew. Chem.* **1998**, *110*, 2003–2006

Keywords: heterogeneous catalysis • nitric oxides • reductions • silver • zeolites

- [1] K. C. Taylor, *Catal. Rev. Sci. Eng.* **1993**, *35*, 457–481.
- [2] M. Shelef, *Chem. Rev.* **1995**, *95*, 209–225.
- [3] S. Sato, Y. Yu-u, H. Yahiro, N. Mizuno, M. Iwamoto, *Appl. Catal.* **1991**, *70*, L1–L5.
- [4] H. Hamada, Y. Kintaichi, M. Sasaki, T. Ito, M. Tabata, *Appl. Catal.* **1990**, *64*, L1–L4.
- [5] Y. Li, T. L. Slager, J. N. Armor, *J. Catal.* **1994**, *150*, 388–399.
- [6] D. B. Lukyanov, E. A. Lombardo, G. A. Sill, J. L. d'Itri, W. K. Hall, *J. Catal.* **1996**, *163*, 447–456.
- [7] J. L. d'Itri, W. M. H. Sachtler, *Catal. Lett.* **1992**, *15*, 289–295.
- [8] H. Hamada, *Catal. Surv.* **1997**, *1*, 53–60.
- [9] a) P. A. Jacobs, J. B. Uytterhoeven, H. K. Beyer, *J. Chem. Soc. Faraday Trans. 1* **1977**, *73*, 1755–1762; b) P. A. Jacobs, *Stud. Surf. Sci. Catal.* **1986**, *29*, 357–414.
- [10] a) M. Iwamoto, *Stud. Surf. Sci. Catal.* **1994**, *84*, 1395–1410; b) T. Miyadera, *Appl. Catal. B* **1993**, *2*, 199–205.
- [11] a) K. Masuda, K. Tsujimura, K. Shinoda, T. Kato, *Appl. Catal. B* **1996**, *8*, 33–40; b) N. Aoyama, K. Yoshida, A. Abe, T. Miyadera, *Catal. Lett.* **1997**, *43*, 249–253.
- [12] K. C. C. Kharas, H. J. Robota, D. J. Liu, *Appl. Catal. B* **1993**, *2*, 225–237.
- [13] R. A. Sheldon, J. K. Kochi, *Metal-Catalyzed Oxidations of Organic Compounds*, Academic Press, New York, **1981**.
- [14] R. Burch, P. J. Millington, A. P. Walker, *Appl. Catal. B* **1994**, *4*, 65–94.
- [15] a) H. Shechter, J. J. Gardikes, A. H. Pagano, *J. Am. Chem. Soc.* **1959**, *81*, 5420–5423; b) H. Shechter, J. J. Gardikes, T. S. Cantrell, G. V. D. Tiers, *J. Am. Chem. Soc.* **1967**, *89*, 3005–3014.
- [16] P. Noble, Jr., F. G. Borgardt, W. L. Reed, *Chem. Rev.* **1964**, *64*, 19–57.
- [17] C. Yokoyama, M. Misono, *J. Catal.* **1994**, *150*, 9–17.
- [18] J. March, *Advanced Organic Chemistry*, 3rd ed., Wiley, New York, **1985**, pp. 739–740.
- [19] R. T. Morrisson, N. R. Boyd, *Organic Chemistry*, 3rd. ed. Allyn and Bacon, Boston, **1973**, pp. 763–767.
- [20] M. Iwamoto, A. M. Hernandez, T. Zengyo, *Chem. Commun.* **1997**, 37–38.

Determination of the Orientation of a Distant Bond Vector in a Molecular Reference Frame by Cross-Correlated Relaxation of Nuclear Spins**

Bernd Reif, Henning Steinhagen, Bernd Junker, Michael Reggelin, and Christian Griesinger*

Dedicated to Professor Richard R. Ernst on the occasion of his 65th birthday

Recently, a new class of structural restraints has been introduced that allows the measurement of projection angles between internuclear vectors from relaxation rates of double-quantum (DQ) and zero-quantum (ZQ) coherences.^[1] This relaxation mechanism is induced by cross-correlation of two individual dipolar coupling tensors. Angular restraints can also be obtained by the measurement of relaxation rates of DQ and ZQ coherences that are induced by the cross-correlation of one dipolar coupling and a chemical shift tensor.^[2,3] So far applications have addressed only the measurement of such rates in fully ¹³C/¹⁵N-labeled biomacromolecules. We show here by comparison with a crystal structure that angles between H–H and C–H bond vectors that are separated in space by 7 Å in a small organic molecule can be determined with an accuracy of a few degrees. It is further shown that by measuring two such relaxation rates it is possible to determine the orientation of one vector in the frame of reference of the two other vectors. For sensitivity reasons we had to introduce ¹³C labeling in part of the molecule. The accuracy and precision of the measurement established in this publication will be used in a forthcoming paper to derive long-range structural information for a catalytic intermediate that cannot be crystallized.

In two pairs of nuclei (A¹–A² and B¹–B²) cross-correlated relaxation rates Γ_{A¹A²B¹B²} of DQ and ZQ coherences between nuclei A¹ and B¹ can be measured provided the DQ and ZQ coherence between these nuclei can be excited, the scalar coupling between A¹ and A² as well as between B¹ and B² is resolved, and the main relaxation source for A¹ (B¹) is the dipolar coupling to A² (B²). If we identify the nuclei A¹, A², B¹, and B² according to Table 1 and Figure 1 with (A¹,A²) = (H²⁶,H²⁵) or (H²³,H²⁴) and (B¹,B²) = (C³,H³) all the above requirements are fulfilled by the η³-allylpalladium complex **1**.

[*] Prof. Dr. C. Griesinger, Dr. B. Reif, Dipl.-Chem. B. Junker, Priv.-Doz. Dr. M. Reggelin
Fachbereich Chemie der Universität
Marie-Curie-Strasse 11, D-60439 Frankfurt/Main (Germany)
Fax: (+49)69-7982-9128
E-mail: cigr@krypton.org.chemie.uni-frankfurt.de (C.G.)
re@krypton.org.chemie.uni-frankfurt.de (M.R.)

Dr. H. Steinhagen
Institut für Organische Chemie der Universität Heidelberg (Germany)

[**] Support by the Fonds der Chemischen Industrie and the DFG (B.R. and B.J.) is gratefully acknowledged. H.S. is indebted to Prof. G. Helmchen, Universität Heidelberg, for support. The crystal structure of **1** has been determined by Dr. F. Rominger, Universität Heidelberg. Continuous support by Dr. W. Bermel and Dr. T. Keller, Bruker Karlsruhe, is gratefully acknowledged. All measurements have been done at the "Large Scale Facility for Biomolecular NMR at the University of Frankfurt".

Table 1. Comparison of the angle determined by NMR experiment and crystal structure analysis.

	A ¹	A ²	B ¹	B ²	$\Gamma_{A^1A^2,B^1B^2}^c$	$\theta_{A^1A^2,B^1B^2}^{\text{NMR}}$	$\theta_{A^1A^2,B^1B^2}^{\text{X-ray}}$
DQ/ZQ ₁ ^[a]	H ²⁶	H ²⁵	C ³	H ³	(+0.33 ± 0.30) Hz	$\theta_1 = 52^\circ, 128^\circ, 3^\circ$ ^[b]	54 ^{°[c]}
DQ/ZQ ₂ ^[a]	H ²³	H ²⁴	C ³	H ³	(+1.60 ± 0.10) Hz	$\theta_2 = 41^\circ, 139^\circ, 1^\circ$ ^[b]	140 ^{°[c]}
SQ ^[d]	H ²⁶	H ²⁵	H ²⁶	C ²⁶	(−0.60 ± 0.05) Hz	–	60 ^{°[c]}

[a] Nuclear assemblies for the DQ and ZQ coherences and the SQ coherence described in the text. [b] The angles were determined from the measured relaxation rates according to Equation (3). [c] The projection angles were taken from the crystal structure. [d] The determined rates.

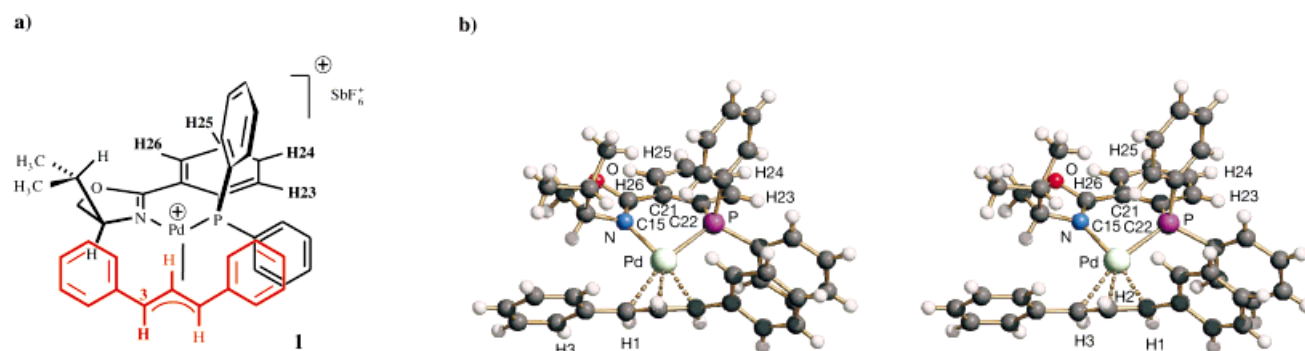


Figure 1. a) Structural formula and b) stereoview of the crystal structure of the η^3 - π -allylpalladium complex cation **1**. 1,3-Diphenyl[¹³C₃]propenol was prepared from [¹³C₁]benzaldehyde, benzene, and [¹³C_{1,2}]-acetylchloride^[8] and was converted into 1,3-diphenyl[¹³C₃]propenylpalladium chloride according to the literature procedure.^[9] Reaction with the corresponding phosphanyloxazoline ligand yields **1**.^[9]

This complex constitutes the catalytic resting state of the allylic substitution that is catalyzed by palladium complexes with chiral phosphanyloxazoline ligands.^[4, 5]

One of the aforementioned cross-correlated relaxation rates is $\Gamma_{H^{26}H^{25},C^3H^3}^c$ and originates from the cross-correlation of the C³–H³ and the H²⁵–H²⁶ dipolar couplings. This relaxation rate is measured on the DQ or ZQ coherence of C³ and H²⁶ and contains structural information according to Equation (1).

$$\Gamma_{H^{26}H^{25},C^3H^3}^c = \frac{\gamma_H\gamma_{13C}}{(r_{C^3,H^3})^3} \frac{\gamma_H\gamma_{1H}}{(r_{H^{26},H^{25}})^3} \left(\frac{\hbar\mu_0}{4\pi} \right)^2 P_2(\cos\theta_{H^{26}H^{25},C^3H^3}) J(0) \quad (1)$$

$$\text{with } J(\omega) = \frac{2}{5} \frac{\tau_c}{1 + (\omega\tau_c)^2} \text{ and } P_2(x) = (3\cos^2 x - 1)/2$$

Here, γ_X denotes the gyromagnetic ratio of nucleus x , and $r_{X,Y}$ is the distance between the nuclei (X,Y). $\theta_{H^{26}H^{25},C^3H^3}^c$ (θ_1) is the projection angle of the C³–H³ and the H²⁵–H²⁶ vectors. The formula for the cross-correlated relaxation between the C³–H³ and the H²⁴–H²³ vectors is analogous. Both projection angles θ_1 and $\theta_{H^{23}H^{24},C^3H^3}^c$ (θ_2) can be used to define the orientation of the allylic moiety with respect to the aromatic ring (C²¹–C²⁶) despite the large intervector distance of approximately 7 Å (Figure 1).

The excitation of the DQ and ZQ coherences between H²⁶ (DQ/ZQ₁, Table 1) or H²³ and C³ (DQ/ZQ₂, Table 1) is achieved by relayed coherence transfer from the protons H²⁶ and H²³, respectively, through the ³¹P atom to the C³ carbon atom (Figure 2). The respective coupling constants are $^4J(H^{26},P) \approx 4$ Hz, $^3J(H^{23},P) = 7.0$ Hz, and $^3J(C^3,P) = 27$ Hz. The H²⁶–C³ DQ and ZQ coherences show a doublet of

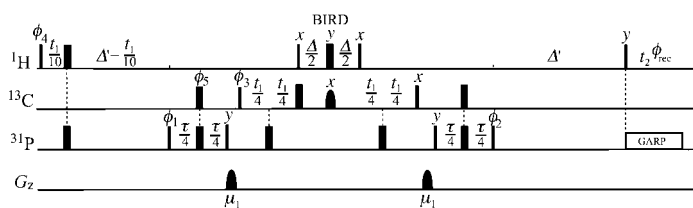


Figure 2. Real-time DQ/ZQ-HPC correlation experiment. Coherence transfer is accomplished by H,P-transfer in a HMQC-type fashion and P,C-transfer in a HSQC-type fashion. The DQ and ZQ coherences are recorded simultaneously and obtained by subtracting spectra acquired with $\phi_3 = \phi_4 = 0^\circ, 180^\circ$ and adding the spectra acquired with $\phi_3 = \phi_4 = 90^\circ, 270^\circ$. Quadrature detection for both DQ and ZQ evolution time is achieved by States TPPI on ϕ_3 and ϕ_5 . $t_1^{\text{max}} = 140$ ms. Decoupling of the proton in the position *meta* to H²⁶ or H²³ is achieved by continuous-wave irradiation with a field strength of $\gamma B_1/2\pi = 6$ Hz. The selective ¹³C BIRD pulse (0.45 ms) serves to refocus all couplings to C³ during the evolution time. The total duration between the first excitation pulse and the detection is $1/3J(H,H) = 128.2$ ms. $\Delta' = 40.5$ ms. In the experiment for H²³ (H²⁶): number of scans = 16 (128), number of t_1 experiments = 320 (142), spectral width in $\omega_1/2\pi = 1000$ Hz (500 Hz). The total duration of the experiment was 4.3 h (15.2 h).

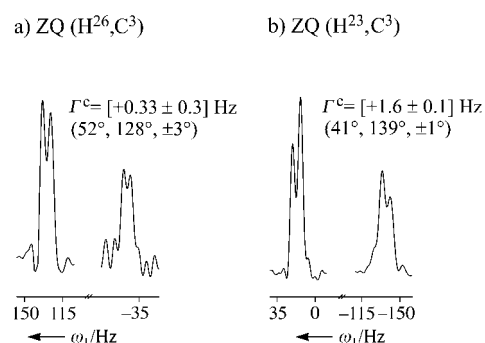


Figure 3. ω_1 traces from the ZQ spectrum of the DQ/ZQ-HPC experiment (Figure 2) applied to **1** (approximately 88 mM) at -60°C in [^D₈]THF. Slices taken at a) H²⁶ and b) H²³ are derived from the H²⁶,C³ and H²³,C³ ZQ coherences. The two doublets from the $^1J(C^3,H^3)$ and the $^3J(H^{26},H^{25})$ coupling for H²⁶ (a) and the $^3J(H^{23},H^{24})$ coupling for H²³ (b) are plotted separately. The cross-correlated relaxation rates and derived angles are also given.

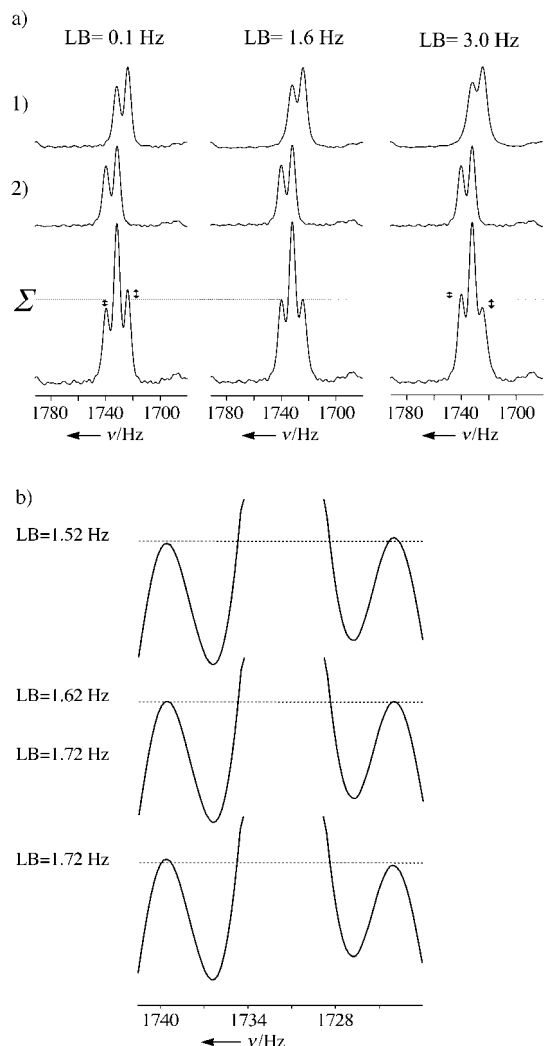


Figure 4. a) Extraction routine for the cross-correlated relaxation on the example of the high-field component of the SQ spectrum of H^{26} (see Figure 5b). The two components in the doublet, which we call $\alpha\alpha$ for the low-field line and $\alpha\beta$ for the high-field line, have a frequency difference of J and reflect the same line shape $\mathcal{F}(\omega)$ except for the Lorentzian contribution:

$$\mathcal{L}(\omega, \Gamma_{\alpha\alpha} - \Gamma_{\alpha\beta}) = \frac{(\Gamma_{\alpha\alpha} - \Gamma_{\alpha\beta})^{-1}}{1 + (\omega / \Gamma_{\alpha\alpha} - \Gamma_{\alpha\beta})^2}$$

The ($\alpha\alpha$) line is broader than the ($\alpha\beta$) line. By duplicating the doublet, shifting the duplicate to the low-field side (1) by J , convoluting it with a trial Lorentzian line with linewidth LB , and adding the result to the second doublet at higher field (2) a triplet (Σ) is formed that has identical outer multiplet components if $LB = (\Gamma_{\alpha\alpha} - \Gamma_{\alpha\beta})$. b) The same example shows that the precision is better than 0.1 Hz. The error for Γ has been determined by adding 20 different noise sections from the same trace on top of the multiplets and applying the extraction procedure. The standard deviation of the mean value of $\Gamma_{\alpha\alpha} - \Gamma_{\alpha\beta}$ then defines the errors of the cross-correlated relaxation rate.

doublets due to the homonuclear coupling $^3J(H^{25}, H^{26}) = 7.8$ Hz and the heteronuclear coupling $^1J(H^3, C^3)$ of 154 Hz (Figure 3a). The H^{23}, C^3 DQ and ZQ coherences show an analogous multiplet structure (Figure 3b). The four lines of the doublets of doublets represent the spin states $\alpha\alpha$, $\alpha\beta$, $\beta\alpha$, and $\beta\beta$ of the passive spins A^2 and B^2 . The desired cross-correlated relaxation rate $\Gamma_{A^1 A^2, B^1 B^2}^c$ is then given by Equation (2).^[1,6]

$$\Gamma_{A^1 A^2, B^1 B^2}^c = \frac{1}{4}(\Gamma_{\alpha\alpha} - \Gamma_{\alpha\beta} - \Gamma_{\beta\alpha} + \Gamma_{\beta\beta}) \quad (2)$$

The experiment depicted in Figure 2 is a real-time experiment with a total duration increasing with t_1 incrementation. In contrast to a constant-time experiment the cross-correlated relaxation rates have to be extracted from the different linewidths of the multiplet. These differences in linewidths can be determined by fitting the $\alpha\alpha$ line to the $\alpha\beta$ line by convolution of the $\alpha\alpha$ line with a Lorentzian line of variable linewidth (Figure 4). The extracted cross-correlated relaxation rates together with the extracted errors are summarized in Table 1.

The size of the cross-correlated relaxation of the DQ and ZQ coherences was calibrated by measuring the cross-correlated relaxation rate of the H^{26} single quantum coherence (SQ_1 , Table 1), which is determined by a dipolar coupling of the single bonded H^{26}, C^{26} and of the *ortho* H^{26}, H^{25} pair (Figure 5). The corresponding cross-correlated relaxation rate $\Gamma_{H^{26} C^{26}, H^{26} H^{25}}^c$ is given by Equation (3).

$$\Gamma_{H^{26} C^{26}, H^{26} H^{25}}^c = \frac{\gamma_H \gamma_C}{(r_{H^{26} C^{26}})^3} \frac{\gamma_H \gamma_H}{(r_{H^{26} H^{25}})^3} \left(\frac{\hbar \mu_0}{4\pi} \right)^2 P_2(\cos \theta_{H^{26} C^{26}, H^{26} H^{25}}) [J(0) + \frac{3}{4} J(\omega_H)] \quad (3)$$

For a correlation time τ_c of 1.8 ns as found at 600 MHz and -60°C for the 88 mM solution of **1** in $[D_8]\text{THF}$, $J(0) + 3/4 J(\omega_H) = 1.06 J(0)$.

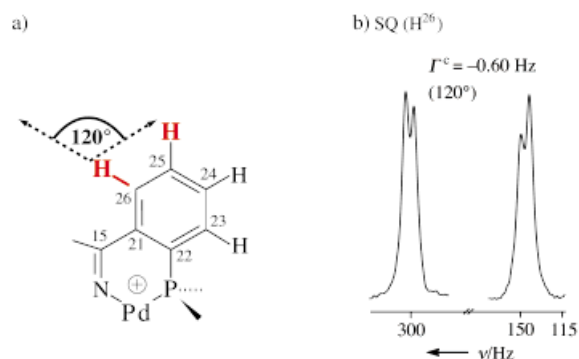


Figure 5. a) The $C^{26}-H^{26}-H^{25}$ moiety for which the cross-correlated relaxation between the $C^{26}-H^{26}$ and the $H^{26}-H^{25}$ dipoles is measured. b) The ^{13}C -filtered 1D ^1H spectrum of H^{26} recorded without refocusing and without ^{13}C decoupling showing the expected doublet of doublets from the $^1J(C^{26}, H^{26})$ and the $^3J(H^{26}, H^{25})$ coupling constants. The high-field doublet has been inverted in sign.

To convert the cross-correlated relaxation rates into direction cosines, the ratio of the cross-correlated relaxation rates of the DQ and ZQ coherences is divided by the rate of the SQ coherence. This value of the desired direction cosines assumes isotropic reorientation, no appreciable effects from internal motion, and identical C–H bond distances in the allyl moiety and the aromatic ring. By using Equations (1) and (3) we arrive at a value of the directional cosines [Eq. (4)].

$$\frac{\Gamma_{H^{26} H^{25}, C^3 H^3}^c}{\Gamma_{H^{26} H^{25}, H^{26} C^{26}}^c} = \frac{(r_{H^{26} C^{26}})^3 P_2(\cos \theta_{H^{26} H^{25}, C^3 H^3})}{(r_{C^3 H^3})^3 P_2(\cos \theta_{H^{26} H^{25}, H^{26} C^{26}})} 1.06 \quad (4)$$

A comparison of the calculated values with those derived from the X-ray structure is given in Table 1. The angles are the same within $\pm 3^\circ$. The accuracy is quite remarkable and

indicates the crystal and the solution structure of complex **1** are identical. In addition, the NMR measurement is very precise; the angles derived here are in the order of 45° where the cross-correlated relaxation rates are most sensitive to the angle. The SQ cross-correlated relaxation rate could also be used for the calibration of the absolute cross-correlated relaxation rates.

In the molecular frame of the aromatic ring ($C^{21}-C^{26}$) the two direction cosines of $C^3 \rightarrow H^3$ relative to $H^{25} \rightarrow H^{26}$ and $H^{24} \rightarrow H^{23}$ define two cones whose intersections determine the orientation of the C^3-H^3 vector (Figure 6). The cartesian coordinates of these vectors are given by Equation (5).

$$x = \cos\theta_1, y = \frac{\cos\theta_2 - \cos\theta_0 \cos\theta_1}{\sin\theta_0}, z = \pm \sqrt{1 - (x^2 + y^2)} \text{ with } |y| < 1 \quad (5)$$

Figure 6 shows these vectors in two graphical representations; Figure 6a is a perspective schematic view and Figure 6b

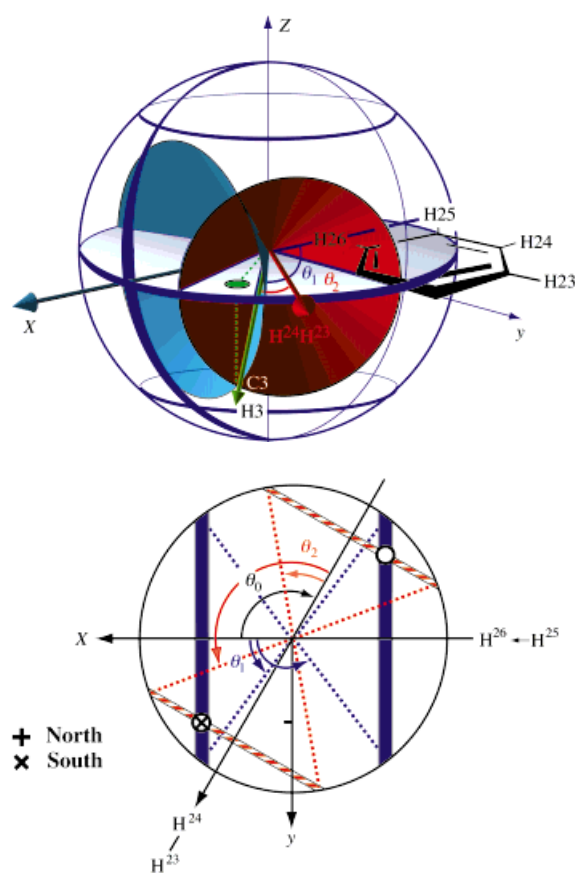


Figure 6. Orientation of the C^3-H^3 vector in the molecular frame of the aromatic ring ($C^{21}-C^{26}$) in a) a 3D representation and b) a polar projection. In both (a) and (b) the two directional cosines from $\Gamma_{H^{25}H^{26}, C^3H^3}^{\infty}$ ($\theta_1 = 52, 128, \pm 3^\circ$) and $\Gamma_{H^{24}H^{23}, C^3H^3}^{\infty}$ ($\theta_2 = 41, 139, \pm 1^\circ$) define two cones for the $C^3 \rightarrow H^3$ vector along the $H^{25} \rightarrow H^{26}$ bond direction (x axis) and the $H^{24} \rightarrow H^{23}$ bond direction ($+(1/2)x + (\sqrt{3}/2)y$ axis), respectively. The two angles θ_1 and θ_2 are also given. The intersection of the cones define the $C^3 \rightarrow H^3$ vector orientation (only one out of the four possibilities is shown in (a)). b) The intersection of each cone with the sphere shows up in the polar representation as two lines in the north and south hemispheres that are perpendicular to the symmetry axis of the cone and intersecting that symmetry axis at $\pm \cos\theta_1$ and $\pm \cos\theta_2$, respectively. The error in $\cos\theta_{1,2}$ is represented by the width of the lines. The intersections of the cones defines two south and two north orientations of the C^3-H^3 vector (\odot). The coordinates are given in the text. The orientation found in the high-resolution crystal structure is marked with an \otimes .

a stereographic projection.^[7] For both Figures $H^{25} \rightarrow H^{26}$ is assumed to lie along the x axis and $H^{24} \rightarrow H^{23}$ along the $(+(1/2)x + (\sqrt{3}/2)y)$ axis). The z axis is assumed to be perpendicular to the x and y axes in a right-handed coordinate system. The angle measured from $H^{25} \rightarrow H^{26}$ to $H^{24} \rightarrow H^{23}$ is $\theta_0 = 120^\circ$. The two cones defined from the two direction cosines $|\cos\theta_1|$ and $|\cos\theta_2|$ are illustrated in Figures 6a and 6b. Their intersections define the possible orientations of the $C^3 \rightarrow H^3$ vector. From the fact that there is no information from the NMR data on the sign of the z -component of the $C^3 \rightarrow H^3$ vector and because of the ambiguity of the $3\cos^2\theta - 1$ dependence, four possible coordinates of the $C^3 \rightarrow H^3$ vector are possible: $(x, y, z) = (0.588, 0.545, \pm 0.599)$ and $(-0.588, -0.545, \pm 0.599)$. The one found in the X-ray structure is $(x, y, z) = (0.616, 0.516, -0.595)$ and matches with the second orientation found from NMR measurements.

In conclusion, we have measured the orientation of internuclear vectors in a small organic molecule over a distance that is large by NMR standards. In the favorable case encountered here the accuracy and precision of the measurement is better than 3° , as shown by comparison with a high-resolution crystal structure. The angular information derived from NMR spectroscopy allows the orientation of two molecular moieties to be defined relative to each other. It is apparent that no other structural parameter used in solution-state NMR spectroscopy would have been able to provide this information. Encouraged by the accuracy and precision of the measurement, we are currently working on using this method to derive information on the catalytic intermediate that has been found in the palladium complex catalyzed allylic transfer and which cannot be crystallized.^[4c]

Received: January 16, 1998 [Z11370IE]
German version: *Angew. Chem.* **1998**, *110*, 2006–2009

Keywords: NMR spectroscopy • palladium • relaxation • structure elucidation

- [1] a) B. Reif, M. Hennig, C. Griesinger, *Science* **1997**, *276*, 1230; b) M. J. J. Blommers, W. Jahnke, *Angew. Chem.* **1998**, *110*, 470; *Angew. Chem. Int. Ed.* **1998**, *37*, 456.
- [2] B. Brutscher, N. R. Skrynnikov, T. Bremi, R. Brüschweiler, R. R. Ernst, *J. Magn. Reson.* **1998**, *130*, 346.
- [3] D. Yang, R. Konrat, L. E. Kay, *J. Am. Chem. Soc.* **1997**, *119*, 11938
- [4] a) G. J. Dawson, C. G. Frost, J. M. J. Williams, S. J. Coote, *Tetrahedron Lett.* **1993**, *34*, 3149; b) P. S. Pregosin, R. Salzmänn, A. Togni, *Organometallics* **1995**, *14*, 842; c) H. Steinhausen, M. Reggelin, G. Helmchen, *Angew. Chem.* **1997**, *109*, 2199; *Angew. Chem. Int. Ed. Engl.* **1997**, *36*, 2108.
- [5] J. Sprinz, G. Helmchen, *Tetrahedron Lett.* **1993**, *34*, 1769; P. von Matt, A. Pfaltz, *Angew. Chem.* **1993**, *105*, 614; *Angew. Chem. Int. Ed. Engl.* **1993**, *32*, 566; J. Sprinz, M. Kiefer, G. Helmchen, M. Reggelin, G. Huttner, O. Walter, L. Zsolnai, *Tetrahedron Lett.* **1994**, *35*, 1523
- [6] a) B. Reif, A. Diener, M. Hennig, M. Maurer, C. Griesinger, unpublished results; b) "Modern Techniques in Protein NMR": C. Griesinger, M. Hennig, J. P. Marino, B. Reif, C. Richter, H. Schwalbe in *Biological Magnetic Resonance Series, Vol. 16* (Eds.: N. R. Krishna, L. J. Berliner), Plenum, London, **1998**, in press.
- [7] M. Hamermesh, *Group Theory and Its Application to Physical Problems*, Addison-Wiley, USA, **1962**.
- [8] a) J. V. Sinisterra, A. Garcia-Raso, J. A. Cabello, J. M. Marinas, *Synthesis* **1984**, *6*, 502; b) *Organikum*, (Ed.: J. A. Barth), 19th Ed., Deutscher Verlag der Wissenschaften, Leipzig, **1993**
- [9] P. R. Auburn, B. Bosnich, P. B. Mackenzie, *J. Am. Chem. Soc.* **1985**, *107*, 2033.